Ocean and Coastal Management 163 (2018) 478–484

Contents lists available at ScienceDirect

Ocean and Coastal Management

journal homepage: www.elsevier.com/locate/ocecoaman

Puerto Rico sea level trend in regional context

Mark R. Jury[a,b,*]

[a] Physics Dept, Univ of Puerto Rico, Mayagüez, PR, 00681, USA
[b] Geography Dept, Univ of Zululand, KwaDlangezwa, 3886, South Africa

ARTICLE INFO

Keywords:
Climate change
Sea level rise
Puerto Rico
Beach erosion

ABSTRACT

Sea level (SL) is rising in Puerto Rico due to regional influences from weaker trade winds, in addition to global influences of thermal expansion and polar ice melt. The linear increase of SL has steepened in recent decades from +0.175 to +0.725 cm/yr. The faster rate of SL rise is partly attributed to diminishing ice volume ($r = -0.80$), notwithstanding a recent decline in the Atlantic Multi-decadal Oscillation. A sophisticated point-to-field regression analysis ($N = 5980$) demonstrates that daily fluctuations of SL in Puerto Rico are significantly enhanced by locally warmer sea temperatures via reduced evaporation, and correspond with lower air pressure accompanying late summer storms. These features point to regional air-sea interactions that affect SL rise over and above the background global signal. Extrapolating these trends, a rise of more than 0.3 m is expected by 2050.

1. Introduction

Coastal zones are dynamic and productive, but susceptible to erosion from rising sea level (SL) (Potter, 1996; Clark, 1997; Huang, 1997; Klein and Nicholls, 1999), especially Caribbean islands with their diminutive size and dense population (184 persons/km^2, IPCC, 2007; United Nations, 2016) and reliance on marine resources (Nicholls, 1998; IPCC, 2013). The Caribbean Sea is framed by South and Central America, the chain of Antilles Islands, and Atlantic Ocean. The island of Puerto Rico is centrally positioned (18ºN, 66ºW) and experiences steady trade winds and temperatures, and has a deep ocean thermocline (Murphy et al., 1999; Andrade and Barton, 2000). Atlantic water infiltrates the Caribbean Sea through the southeastern Antilles (Johns et al., 2002; Gyory et al., 2005), bearing fresh water from South American rivers. Currents flow westward ~0.5 m/s in latitudes 13-17ºN, eventually joining the Gulf Stream (Hernandez-Guerra and Joyce, 2000; Fratantoni, 2001; Johns et al., 2002; Wajsowicz, 2002).

While Caribbean climate processes and fluctuations have been revealed (Alvera-Azcárate et al., 2009), regional influences on SL trends are less informed. The effects of rising greenhouse gas emissions and warming temperatures may be compounded by local trends in the atmospheric circulation (IPCC, 2013; Jury, 2015). Reconstructed global SL records show a 0.19 cm/yr rate of rise in the 20th century (Church and White, 2011; Hamlington et al., 2011). As anthropogenic climate change accelerates the SL trend (Kenigson and Han, 2014), regional variations arise from the underlying geology, changes in the ocean thermohaline circulation (Yin et al., 2009; Hu et al., 2011; Boon, 2012; Ezer and Corlett, 2012; Sallenger et al., 2012; Ezer et al., 2013; Kopp, 2013), coupled low-frequency climate oscillations (Chambers et al., 2012; Liu, 2012; Booth et al., 2012; Scafetta, 2013; Zhang et al., 2013; Knudsen et al., 2014), and the artificial dependence of trend on record length (Baart et al., 2011). This work seeks to identify the factors underlying local SL rise, and is motivated by aerial surveys in Puerto Rico that reveal a ~1 m/yr narrowing of sandy beaches in recent decades (Thieler et al., 2007), The over-topping of dunes and inundation of aquifers will harm infrastructure, water supplies and tourism revenue ($50 B, Turner, 2015).

2. Data and methods

The SL is analyzed using quality controlled daily harbour measurements from National Oceanic and Atmospheric Administration (NOAA) gauges at San Juan 18.46°N, 66.12°W and Parguera 17.97°N, 67.05°W (PSMSL, 2013) on the northeast and southwest coast of Puerto Rico, respectively (Fig. 1a). The two time series are averaged to create a single record from 1955 to 2015 with < 1% missing data (mainly Jun 88 – Feb 89). Monthly averages are calculated and a low pass polynomial filter (Cleveland and Devlin, 1988, Trouet and VanOldenborgh, 2013) is applied to remove periods ≤ 12 months and fill gaps. SL trends are estimated by least squares regression within MS-excel, using default 1st and 2nd order schemes. Wavelet spectral energy is calculated in the two SL records at periods of multi-day and multi-year.

---

[*] Physics Dept, Univ of Puerto Rico, Mayagüez, PR, 00681, USA.
E-mail address: mark.jury@upr.edu.

https://doi.org/10.1016/j.ocecoaman.2018.08.006
Received 31 March 2018; Received in revised form 23 April 2018; Accepted 1 August 2018
0964-5691/

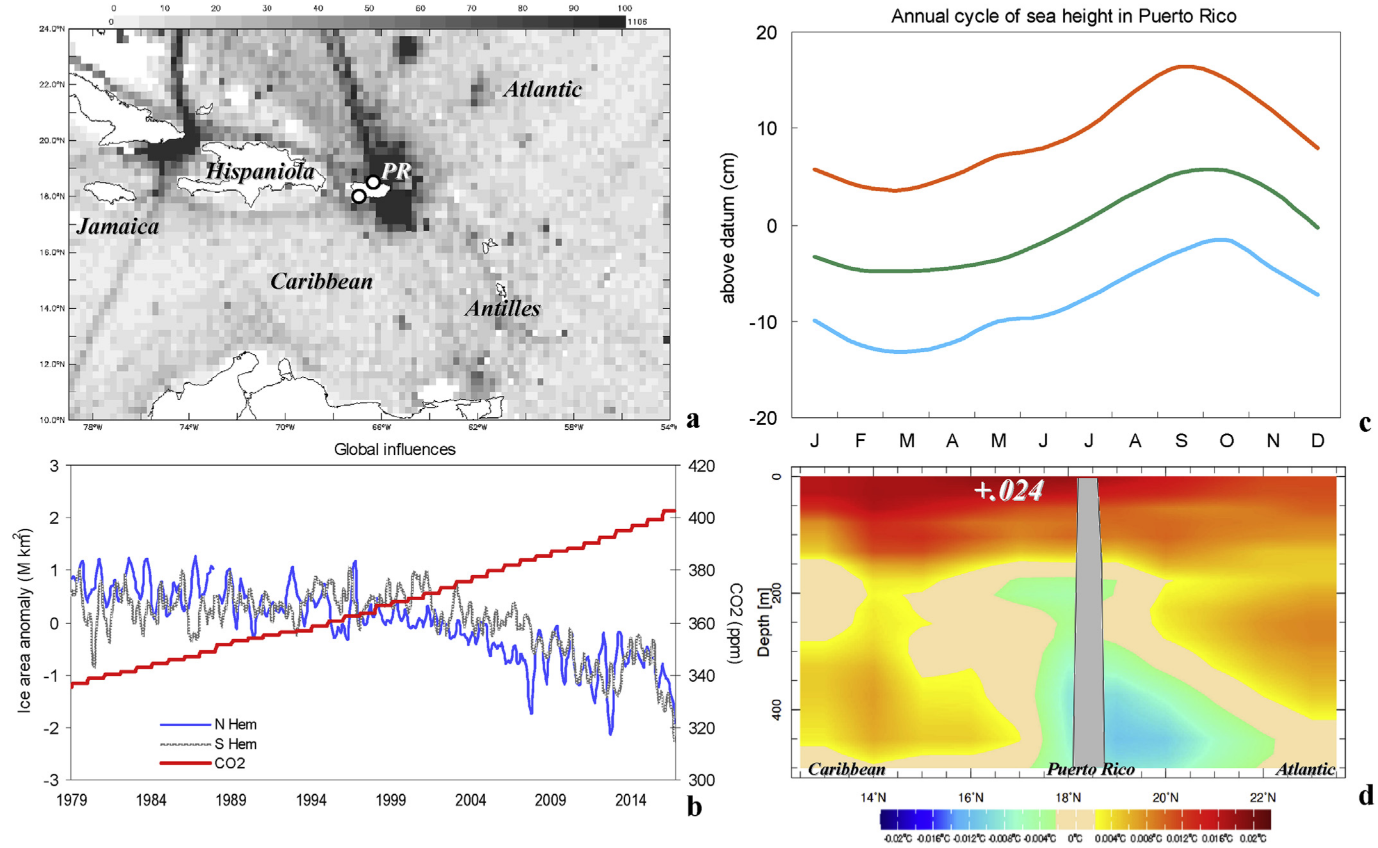

Fig. 1. (a) Ship reporting density for sub-surface temperature, with daily-monthly SL gauges (open dots) on the coast of Puerto Rico (PR). (b) Globally averaged annual CO2 concentration record and satellite-derived anomaly of (northern and southern) polar ice area (IPCC, 2013). (c) Mean annual cycle of SL with upper/lower 2.5% occurence. (d) Linear trend in subsurface ocean temperature averaged 64–68W from GODAS and SODA3 reanalysis; with Puerto Rico shaded.

Sea temperature warming in the Caribbean (10–24°N, 79-54°W) is analyzed over a depth section averaged 64°-68°W. The raw daily and filtered SL records are regressed onto field data on: sea surface height, outgoing longwave radiation (OLR) and sea surface temperature (SST) from satellite (Lee et al., 2007; Reynolds et al., 2007); and sea level pressure (SLP), sea surface temperature (SST), salinity, winds, and evaporation from ocean and atmosphere reanalyses: GODAS/SODA3 (Penny et al., 2015) and MERRA2 (Rienecker et al. 2011; Molod et al., 2015). Fig. 1a illustrates the data density underpinning these reanalyses (from WOA, 2013). The raw daily point-to-field correlations span the scatterometer era 1999–2015 (N = 5980), whereas the 12-month filtered SL correlations cover the satellite-reanalysis era 1980–2015 (N = 482). Serial auto-correlation and filtering reduce the degrees of freedom by a factor of ~10. The filtered SL record was regressed onto a variety of climate indices 1955+ (eg. Pacific Nino3 SST) and onto climate change variables 1980+ (eg. NSIDC polar ice, NODC ocean heat content, CDIAC global CO2 concentration).

Future SL projections to 2050, using the rcp8 scenario (VanVuuren et al. 2011), derive from CMIP-5 Hadley Centre v2 earth system model simulation (Collins et al. 2011) that corresponds with recent SL trends observed in Puerto Rico. Other CMIP-5 simulations show less agreement, for obscure reasons that could relate to feedback between over-land polar ice melt and rising greenhouse gas concentrations amongst other factors.

3. Results

3.1. Global context

Global influences on SL include thermal expansion and (over-land) ice melt, driven by rising greenhouse gases such as CO2, whose concentration is plotted together with satellite measurements of polar ice area in Fig. 1b. In the absence of geological uplift or subsidence, station records should follow the background global trends. The filtered PR SL time series correlates as follows: −0.37 with NSIDC N. Hem ice area, −0.30 with NSIDC S. Hem ice area, 0.45 with global CO2, -0.80 with NSIDC N. Hem ice volume (cf. Fig. 2d), and 0.42 with NODC global upper ocean (0–700 m) heat content in the period 1980–2015. The correlation with ice volume over Greenland is particularly striking, and indicates that global forces tend to override regional effects. In addition, the Atlantic Multi-decadal Oscillation has shown a decline since 2005 (Frajka-Williams et al., 2017) while PR SL has risen more steeply.

3.2. Annual cycle and section trend

The mean annual cycle of Puerto Rico SL peaks in September–October (Fig. 1c) when SLP is lowest. The SL follows the annual cycle of SST, rising in October and falling in March. These points tend to confirm known thermodynamic/hydrostatic influences, while steric effects tend to be most noteable at shorter time-scales (cf. section 3.4).

Trends in two ocean reanalysis (GODAS, SODA3) averaged over a depth section 64–68W 1980–2015 are illustrated in Fig. 1d. The subsurface temperature trends show considerable warming (> +0.02 °C/yr) in the upper 100 m, and weak cooling below 200 m to the north of Puerto Rico. Westward currents have weakened in Caribbean 16-17ºN (not shown), and the longer residence times for the build-up of surplus heat emerge in the upper layer warming of sea temperatures.